J|A|C|S ARTICLES

Published on Web 07/01/2009

# Reactions of Group III Biheterocyclic Complexes

Colin T. Carver,[‡] Diego Benitez,[§] Kevin L. Miller,[‡] Bryan N. Williams,[‡] Ekaterina Tkatchouk,[§] William A. Goddard III,[§] and Paula L. Diaconescu*[,‡]

*Department of Chemistry & Biochemistry, University of California, Los Angeles, California 90095, and Materials and Process Simulation Center, California Institute of Technology, Pasadena, California 91125*

Received April 7, 2009; E-mail: pld@chem.ucla.edu

***Abstract:*** Group III alkyl complexes supported by a ferrocene diamide ligand (1,1′-fc(NSi$^t$BuMe$_2$)$_2$) have been found to be reactive toward aromatic N-heterocycles such as 1-methylimidazole and pyridines. These reactions were investigated experimentally and computationally. An initial C−H activation event is followed by a coupling reaction to form biheterocyclic complexes, in which one of the rings is dearomatized. In the case of 1-methylimidazole, the biheterocyclic compound could not be isolated and further led to an imidazole ring-opened product; in the case of pyridines, it transformed into an isomer with extended conjugation of double bonds. Mechanisms for both reactions are proposed on the basis of experimental and computational results. DFT calculations were also used to show that an energetically accessible pathway for the ring-opening of pyridines exists.

## Introduction

Hydrodenitrogenation (HDN),[1−6] the decomposition of nitrogen-containing impurities from fuels, is becoming increasingly important as limited oil supplies dictate a shift toward hydrocarbon sources containing larger amounts of N-heterocycles.[6] The breaking of C−N bonds in heterocycles is the most difficult step in HDN processes, requiring reduction of the aromatic ring with $H_2$ prior to the cleavage of the C−N bond.[1−6] Current industrial heterogeneous catalysts for this process operate at 300−500 °C and 200 atm $H_2$, making them rather energy intensive.[1,2] The development of soluble organometallic catalysts[7,8] for C−N bond cleavage may lead to novel processes, which would operate under mild conditions and do not require the reduction of the aromatic rings with hydrogen. In addition, studies of the activation of C−N bonds in heterocycles by organometallic complexes might elucidate the mechanism underlying the heterogeneous HDN processes.

Examples of homogeneous systems[9] that mediate the ring-opening of N-heterocycles are exclusively based on early transition metals such as tantalum,[8,10−15] niobium,[16−19] and titanium,[20,21] with the exception of a rhenium system[22,23] that employs external bases and electrophilic reagents. The strong thorium−oxygen bond can drive the ring-opening of pyridine-N-oxides by thorium bis-cyclopentadienyl complexes.[24] In a previous communication, the ring-opening of imidazole rings was reported to be mediated by scandium and yttrium alkyl complexes[25] supported by a ferrocene diamide ligand (NN$^{fc}$ =

[‡] University of California, Los Angeles.
[§] California Institute of Technology.

(1) Katzer, J. R.; Sivasubramanian, R. *Catal. Rev.-Sci. Eng.* **1979**, *20*, 155–208.
(2) Ho, T. C. *Catal. Rev.-Sci. Eng.* **1988**, *30*, 117–160.
(3) Perot, G. *Catal. Today* **1991**, *10*, 447–472.
(4) Prins, R. In *A Handbook of Heterogeneous Catalysis*; Ertl, G., Knözinger, H., Weitkamp, J., Eds.; VCH Verlagsgesellschaft: Weinheim, Germany, 1997.
(5) Kabe, T.; Ishikawa, A.; Qian, W. *Hydrodesulfurization and Hydrodenitrogenation*; Wiley-VCH: Chichester, UK, 1999.
(6) Furimsky, E.; Massoth, F. E. *Catal. Rev.-Sci. Eng.* **2005**, *47*, 297–489, and references therein.
(7) Sanchez-Delgado, R. A. *Organometallic modelling of the hydrodesulfurization and hydrodenitrogenation reactions*; Kluwer Academic Publishers: Dordrecht, The Netherlands, 2002.
(8) Weller, K. J.; Fox, P. A.; Gray, S. D.; Wigley, D. E. *Polyhedron* **1997**, *16*, 3139–3163, and references therein.
(9) Diaconescu, P. L. *Curr. Org. Chem.* **2008**, *12*, 1388–1405.
(10) Gray, S. D.; Weller, K. J.; Bruck, M. A.; Briggs, P. M.; Wigley, D. E. *J. Am. Chem. Soc.* **1995**, *117*, 10678–10693.
(11) Gray, S. D.; Smith, D. P.; Bruck, M. A.; Wigley, D. E. *J. Am. Chem. Soc.* **1992**, *114*, 5462–5463.
(12) Weller, K. J.; Gray, S. D.; Briggs, P. M.; Wigley, D. E. *Organometallics* **1995**, *14*, 5588–5597.
(13) Weller, K. J.; Filippov, I.; Briggs, P. M.; Wigley, D. E. *Organometallics* **1998**, *17*, 322–329.
(14) Weller, K. J.; Filippov, I.; Briggs, P. M.; Wigley, D. E. *J. Organomet. Chem.* **1997**, *528*, 225–228.
(15) Allen, K. D.; Bruck, M. A.; Gray, S. D.; Kingsborough, R. P.; Smith, D. P.; Weller, K. J.; Wigley, D. E. *Polyhedron* **1995**, *14*, 3315–3333.
(16) Kleckley, T. S.; Bennett, J. L.; Wolczanski, P. T.; Lobkovsky, E. B. *J. Am. Chem. Soc.* **1997**, *119*, 247–248.
(17) Bonanno, J. B.; Veige, A. S.; Wolczanski, P. T.; Lobkovsky, E. B. *Inorg. Chim. Acta* **2003**, *345*, 173–184.
(18) Covert, K. J.; Neithamer, D. R.; Zonnevylle, M. C.; LaPointe, R. E.; Schaller, C. P.; Wolczanski, P. T. *Inorg. Chem.* **1991**, *30*, 2494–2508.
(19) Neithamer, D. R.; Parkanyi, L.; Mitchell, J. F.; Wolczanski, P. T. *J. Am. Chem. Soc.* **1988**, *110*, 4421–4423.
(20) Fout, A. R.; Bailey, B. C.; Tomaszewski, J.; Mindiola, D. J. *J. Am. Chem. Soc.* **2007**, *129*, 12640–12641.
(21) Bailey, B. C.; Fan, H.; Huffman, J. C.; Baik, M. H.; Mindiola, D. J. *J. Am. Chem. Soc.* **2006**, *128*, 6798–6799.
(22) Huertos, M. A.; Perez, J.; Riera, L. *J. Am. Chem. Soc.* **2008**, *130*, 5662–5663.
(23) Huertos, M. A.; Pérez, J.; Riera, L.; Menéndez-Velázquez, A. *J. Am. Chem. Soc.* **2008**, *130*, 13530–13531.
(24) Pool, J. A.; Scott, B. L.; Kiplinger, J. L. *Chem. Commun.* **2005**, 2591–2593.
(25) Carver, C. T.; Diaconescu, P. L. *J. Am. Chem. Soc.* **2008**, *130*, 7558–7559.
(26) Monreal, M. J.; Diaconescu, P. L. *Organometallics* **2008**, *27*, 1702–1706.

  

***Scheme 1.*** Proposed Mechanism for the Ring-Opening of 1-Methylimidazole by the Scandium Alkyl Complex **1$^{Sc}$-THF**

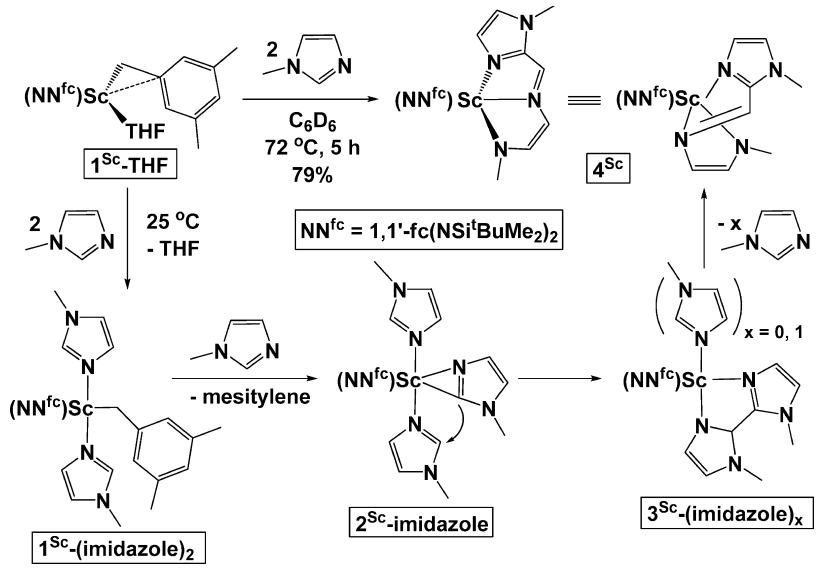


1,1′-fc(NSi$^t$BuMe$_2$)$_2$).[26−37] At the time, the mechanism proposed for this transformation (Scheme 1) involved the C−H activation of one imidazole ring by **1$^{Sc}$-THF**[27] to give **2$^{Sc}$-imidazole**, nucleophilic attack of the imidazolyl carbon of **2$^{Sc}$-imidazole** on one of the coordinated imidazoles to lead to coupling of two rings in **3$^{Sc}$-(imidazole)$_x$** ($x$ = 0, 1, see below),[38] and, finally, ring-opening of the dearomatized ring in the new biheterocyclic structure formed, **3$^{Sc}$-(imidazole)$_x$**, to give the final product **4$^{Sc}$**. The intermediate **3$^{Sc}$-(imidazole)$_x$** could not be isolated, but an analogous coupling product of two pyridine rings was characterized.[25] We had also observed a subsequent reaction of this pyridine-coupled complex, but the reaction gave an intractable mixture of products. In the present paper we report on group III (Sc, Y, Lu) biheterocyclic complexes, based on imidazole and pyridine, that, although share similar structures, lead to different transformations. The ring-opening of imidazole reported previously was not mirrored by these analogous pyridine complexes, which, instead, underwent an isomerization process. In order to determine the mechanistic origin of this difference in reactivity, DFT calculations were carried out on various plausible pathways. The theoretical and experimental results are consistent, establishing the nature of intermediates and transition states and explaining the two distinct outcomes.

## Results and Discussion

**Synthesis and Characterization of Complexes.** The scandium-mediated coupling of pyridine rings to form biheterocyclic structures, in which one of the rings is dearomatized, was expanded to other six-membered aromatic N-heterocycles such as quinoline and isoquinoline (Scheme 2). The presence of a substituent ortho to the heteroatom aids both the C−H activation and the coupling reactions. Similar reactions were also found for the analogous yttrium and lutetium complexes (Scheme 2). The reaction (in $C_6D_6$ or toluene) times vary from 15 min for **6$^{Sc}$-py$^{Ph}$-iqn** to 2 h at room temperature for **6$^{M}$-py$^{Ph}$-iqn** (M = Y, Lu) and likely depend on (a) the probability of the second pyridine to coordinate to the metal center and (b) the release of the steric hindrance that takes place after the coupling event. The displacement of THF and coordination of the second pyridine to **5$^{M}$-pyridine** were not observed, but they must occur before the coupling process takes place. Also, the formation of **5$^{Y}$-qn** or **5$^{Lu}$-qn** (qn = 8-methylquinoline) was not accomplished, although a reaction between **1$^{Y}$-THF** or **1$^{Lu}$-THF** and 8-methylquinoline occurred (those results will be reported elsewhere).

Complexes **6$^{M}$** were characterized by elemental analysis, $^1$H and $^{13}$C NMR spectroscopy, and, in the case of **6$^{Sc}$-py$^{Ph}$-iqn** (iqn = 3-methylisoquinoline), X-ray crystallography (Figure 1; the structural parameters are discussed below). The dearomatization of the second pyridine ring was consistent with peaks observed in the olefinic region [see the Supporting Information for a detailed NMR analysis using 2D heteronuclear multiple bond coherence-gradient pulse (HMBC-gp), 2D heteronuclear

***Scheme 2.*** Coupling of 2-Phenylpyridine or 8-Methylquinoline with 3-Methylisoquinoline Mediated by Group III Metal Centers

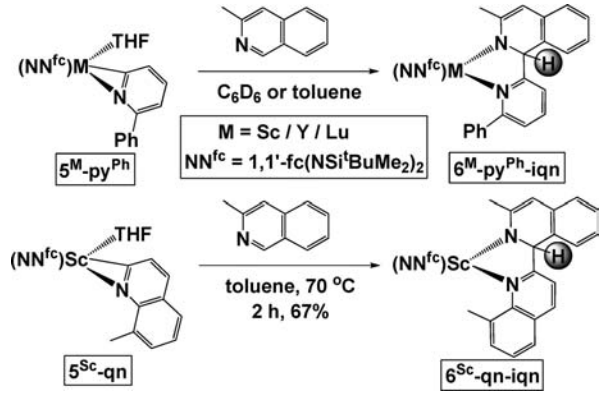


(27) Carver, C. T.; Monreal, M. J.; Diaconescu, P. L. *Organometallics* **2008**, *27*, 363–370.
(28) Monreal, M. J.; Carver, C. T.; Diaconescu, P. L. *Inorg. Chem.* **2007**, *46*, 7226–7228.
(29) Shafir, A.; Arnold, J. *Organometallics* **2003**, *22*, 567–575.
(30) Shafir, A.; Arnold, J. *Inorg. Chim. Acta* **2003**, *345*, 216–220.
(31) Shafir, A.; Power, M. P.; Whitener, G. D.; Arnold, J. *Organometallics* **2001**, *20*, 1365–1369.
(32) Shafir, A.; Arnold, J. *J. Am. Chem. Soc.* **2001**, *123*, 9212–9213.
(33) Ulrich, S. *Z. Anorg. Chem.* **2005**, *631*, 2957–2966.
(34) Siemeling, U.; Auch, T.-C. *Chem. Soc. Rev.* **2005**, *34*, 584.
(35) Siemeling, U.; Auch, T. C.; Kuhnert, O.; Malaun, M.; Kopacka, H.; Bildstein, B. *Z. Anorg. Allg. Chem.* **2003**, *629*, 1334–1336.
(36) Eppinger, J. r.; Nikolaides, K. R.; Zhang-Presse, M.; Riederer, F. A.; Rabe, G. W.; Rheingold, A. L. *Organometallics* **2008**, *27*, 736–740.
(37) Siemeling, U.; Auch, T.-C.; Tomm, S.; Fink, H.; Bruhn, C.; Neumann, B.; Stammler, H.-G. *Organometallics* **2007**, *26*, 1112–1115.
(38) Deelman, B.-J.; Stevels, W. M.; Teuben, J. H.; Lakin, M. T.; Spek, A. L. *Organometallics* **1994**, *13*, 3881–3891.

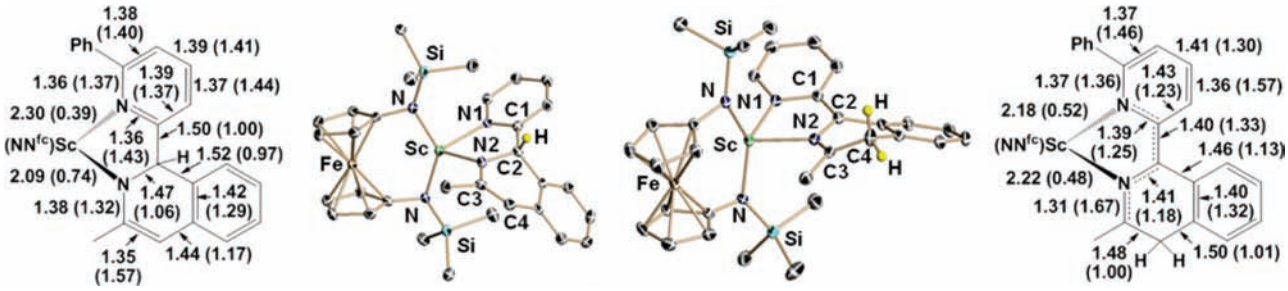


***Figure 1.*** Extreme left and right: Relevant metrical parameters (in Å) from the X-ray crystal structures of **6$^{Sc}$-py$^{Ph}$-iqn** and **7$^{Sc}$-py$^{Ph}$-iqn** and, in parentheses, bond orders calculated by ADF2008.01 from geometry optimizations on the full molecules. Center: ORTEP representations of **6$^{Sc}$-py$^{Ph}$-iqn** and **7$^{Sc}$-py$^{Ph}$-iqn** with ellipsoids drawn at 50% probability ($^t$Bu methyl, pyridine phenyl groups, and irrelevant hydrogen atoms were removed for clarity).

***Scheme 3.*** Isomerization of Biheterocyclic Ligands in **6$^M$** Complexes (M = Sc, Y, Lu)

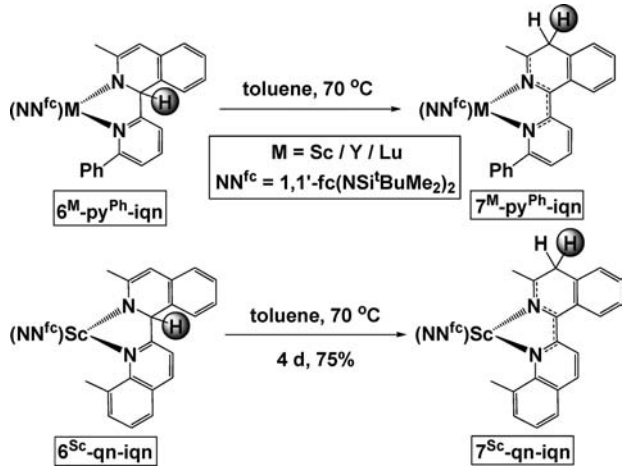


multiple quantum coherence-gradient pulse (HMQC-gp), and distortionless enhancement by polarization transfer (DEPT-135) experiments].[39,40]

In order to test the reactivity of the newly obtained pyridine-coupled products, $C_6D_6$ solutions of the complexes **6$^M$-py$^{Ph}$-iqn** (M = Sc, Y, Lu) were heated at 70 or 85 °C for several days, during which time their color changed from red to green (Scheme 3). All **6$^M$-py$^{Ph}$-iqn** (M = Sc, Y, Lu) compounds transformed to **7$^M$-py$^{Ph}$-iqn** (M = Sc, Y, Lu) in at least 60% conversion. However, only in the case of scandium, **7$^{Sc}$-py$^{Ph}$-iqn** was isolated and purified, owing to solubility differences between **6$^{Sc}$-py$^{Ph}$-iqn** and **7$^{Sc}$-py$^{Ph}$-iqn**. The identity of the products **7$^M$-py$^{Ph}$-iqn** (M = Y, Lu) was established by comparison of their NMR spectra with those of **7$^{Sc}$-py$^{Ph}$-iqn** (see the Supporting Information for details). Crystals of the product **7$^{Sc}$-py$^{Ph}$-iqn** were obtained from a concentrated hexanes/toluene solution; the X-ray crystal structure obtained revealed that the hydrogen atom from the isoquinoline C2 atom migrated to C4 (Figure 1). $^1$H NMR spectroscopy supported this interpretation since a new peak at 3.20 ppm was found for **7$^{Sc}$-py$^{Ph}$-iqn**, consistent with its benzylic character. A thorough investigation of the $^1$H and $^{13}$C NMR spectra of **7$^{Sc}$-qn-iqn** using 2D HMQC-gp and 2D HMBC-gp[39,40] showed that the analogous peak at 3.14 ppm in its $^1$H NMR spectrum corresponds to a peak at 30.0 ppm in its $^{13}$C NMR spectrum. This $^{13}$C NMR peak was assigned to a methylene carbon on the basis of the information obtained from the DEPT-135 spectrum. By contrast, all carbon atoms in **6$^{Sc}$-qn-iqn** were shown by DEPT-135 to be quaternary, methyne, or methyl atoms (see the Supporting Information for a detailed NMR analysis).

The comparison of metrical parameters for the structures of **6$^{Sc}$-py$^{Ph}$-iqn** and **7$^{Sc}$-py$^{Ph}$-iqn** also agrees with the structural assignment for **7$^{Sc}$-py$^{Ph}$-iqn** (Figure 1): the C1−C2 distance between the two heterocyclic rings decreased from 1.505(4) Å in **6$^{Sc}$-py$^{Ph}$-iqn** to 1.398(3) Å in **7$^{Sc}$-py$^{Ph}$-iqn**; the Sc−N1 distance increased from 2.086(2) Å in **6$^{Sc}$-py$^{Ph}$-iqn** to 2.178(2) Å in **7$^{Sc}$-py$^{Ph}$-iqn**, while the Sc−N2 distance decreased from 2.303(2) Å in **6$^{Sc}$-py$^{Ph}$-iqn** to 2.224(2) Å in **7$^{Sc}$-py$^{Ph}$-iqn**. All other distances (Figure 1) and the sum of the angles around C2 of 360.3° are in accord with the delocalization of an electron pair in **7$^{Sc}$-py$^{Ph}$-iqn** over the N1−C1−C2−N2−C3 atoms.

The assigned electronic structure of **7$^{Sc}$-py$^{Ph}$-iqn** is also supported by bond order calculations based on Nalewajski−Mrozek valence indices[41] obtained from geometry optimizations on the full molecules (**6$^{Sc}$-py$^{Ph}$-iqn** and **7$^{Sc}$-py$^{Ph}$-iqn**) using ADF2008.01. These calculations show that the C1−C2 bond order increases from 1.00 in **6$^{Sc}$-py$^{Ph}$-iqn** to 1.33 in **7$^{Sc}$-py$^{Ph}$-iqn**, and the Sc−N1 bond order increases from 0.39 in **6$^{Sc}$-py$^{Ph}$-iqn** to 0.52 in **7$^{Sc}$-py$^{Ph}$-iqn**, while the Sc−N2 bond order decreases from 0.74 in **6$^{Sc}$-py$^{Ph}$-iqn** to 0.48 in **7$^{Sc}$-py$^{Ph}$-iqn**. The bonds over which the electron pair is delocalized in **7$^{Sc}$-py$^{Ph}$-iqn** feature bond orders consistent with aromatic character: 1.25 for N1−C1, 1.18 for C2−N2, and 1.67 for N2−C3 (Figure 1).

The isomerization reaction described here is not limited to the complexes **6$^M$-py$^{Ph}$-iqn** (M = Sc, Y, Lu). The analogous coupled products of 2-phenylpyridine with 2-picoline or 8-methylquinoline with 3-methylisoquinoline, **6$^{Sc}$-qn-pic** or **6$^{Sc}$-qn-iqn**, respectively, also show similar transformations upon heating to form the complexes **7$^{Sc}$-qn-pic** and 7$^{Sc}$-**qn-iqn**, respectively. In the case of **7$^{Sc}$-qn-pic**, the coupling product **6$^{Sc}$-qn-pic** could not be isolated because its formation was competitive with its isomerization. Although **7$^{Sc}$-qn-pic** could not be characterized by single-crystal X-ray diffraction, we were able to obtain a structure for **7$^{Sc}$-qn-iqn** (see the Supporting Information for details). These additional reactions were limited to scandium complexes because intractable mixtures of products were observed for the analogous yttrium and lutetium cases. Other biheterocyclic complexes, analogous to **6$^M$**, could be obtained, but the heating of their solutions also gave intractable mixtures of products. In some of those mixtures, complexes of the type

(39) Derome, A. E. *Modern NMR techniques for chemistry research*; Pergamon: Cambridge, 1988.
(40) Rahman, A.-U. *One and two dimensional NMR spectroscopy* Elsevier: Amsterdam, 1989.
(41) Michalak, A.; DeKock, R. L.; Ziegler, T. *J. Phys. Chem. A* **2008**, *112*, 7256–7263.

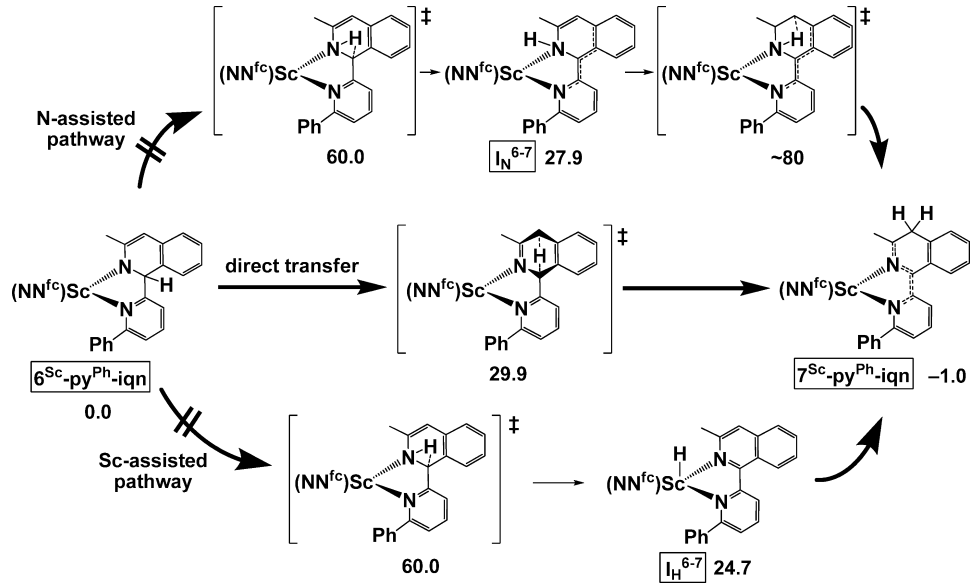


***Figure 2.*** Pathways studied computationally for the isomerization of **$6^{Sc}$-$py^{Ph}$-iqn** to **$7^{Sc}$-$py^{Ph}$-iqn**; all energies given in kcal/mol.

**$7^M$** could be identified by $^1$H NMR spectroscopy, but their separation and isolation were not successful.

**Mechanistic Studies.** Because this previously unreported isomerization process is general for the complexes described here, it became imperative to understand its mechanism. For this purpose, 3-methylisoquinoline was deuterated at the 1-position (deuterium incorporation at the 3-methyl position was also observed),[42] and the compound **$6^{Sc}$-qn-iqn-$d_4$** was prepared. Compound **$6^{Sc}$qn-iqn-$d_4$** was heated at 70 °C, and the formation of **$7^{Sc}$-qn-iqn-$d_4$** was monitored by both $^1$H and $^2$H NMR spectroscopy. A kinetic isotope effect of 4 ± 1 was estimated from the monitoring of the reaction mixtures.

In order to establish whether the isomerization process is intra- or intermolecular, a mixture of **$6^{Sc}$-qn-iqn-$d_4$** and **$6^{Sc}$-$py^{Ph}$-iqn** was heated at 70 °C (eq 1). Inspection by $^1$H and $^2$H NMR spectroscopy showed that there was no deuterium incorporation in **$7^{Sc}$-$py^{Ph}$-iqn**, indicating that the isomerization reaction is an intramolecular process. An intermolecular process would involve the deprotonation of C2 followed by the protonation of C4, and incorporation of deuterium into **$7^{Sc}$-$py^{Ph}$-iqn** would have been observed. The intramolecular nature of the transformation is also supported by two other observations: (1) reactions run in the presence of excess 3-methylisoquinoline did not proceed at a different rate than reactions run in its absence, and (2) the addition of $Et_3N$ to **$6^{Sc}$-qn-iqn** did not influence the rate of the isomerization process.

At the suggestion of a reviewer, the isomerization reactions were also run in the presence of 1,8-diazabicyclo[5.4.0]undec-7-ene (DBU); the complex **$6^{Sc}$-qn-iqn** transforms to **$7^{Sc}$-qn-iqn** at room temperature within 30 min, while for **$6^{Sc}$-$py^{Ph}$-iqn** an equilibrium mixture of 75% **$7^{Sc}$-$py^{Ph}$-iqn** and 25% **$6^{Sc}$-$py^{Ph}$-iqn** was observed at room temperature after 8 h, regardless of whether DBU was used in catalytic (20 mol %) or stoichiometric amount. A crossover experiment between **$6^{Sc}$-$py^{Ph}$-iqn-$d_4$** and **$6^{Sc}$-qn-iqn**, run in the presence of DBU, showed, again, that there is no deuterium incorporation into **$7^{Sc}$-$py^{Ph}$-iqn**. However, the deuterium label was found in various positions of DBU, so the crossover experiment was inconclusive with respect to the nature of the DBU-mediated process. A similar observation has been

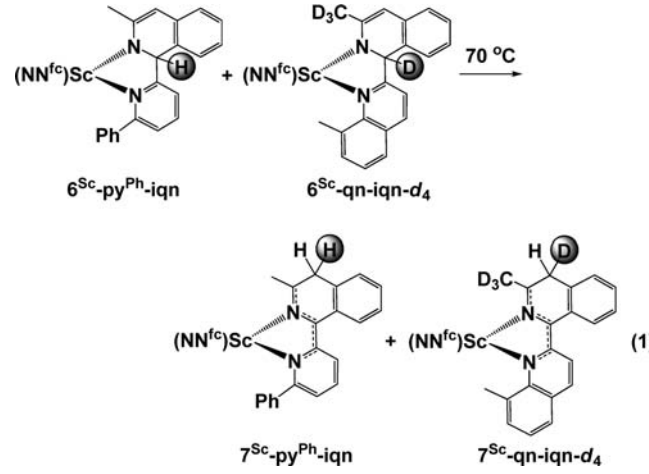


reported for the DBU-catalyzed deconjugation of 7-substituted 3,4-didehydro-2-oxepanones.[43] That study concluded that DBU is a special base and its effect on the reaction was dependent on the presence of the imine N=C bond since similar strength bases did not produce the same results. On the basis of these observations, we conclude that DBU acts as a catalyst, but it may change the mechanism of the isomerization reaction as compared to that of reactions run in its absence (see the Supporting Information for the corresponding NMR spectra).

**Computational Studies.** The mechanism for the isomerization of **$6^{Sc}$-$py^{Ph}$-iqn** to **$7^{Sc}$-$py^{Ph}$-iqn** was explored using density functional theory (DFT). Geometry optimizations were carried out on the full molecules using Jaguar 7.5, and energies were computed at the B3LYP/LACV3P++**(2f)//B3LYP/LACVP** level of theory.[44] Three different intramolecular pathways were examined for the migration of the proton from the isoquinoline C2 to C4: (1) nitrogen-assisted, (2) metal-assisted, and (3) direct transfer (Figure 2). All pathways led to the product **$7^{Sc}$-$py^{Ph}$-**

(42) Rubottom, G. M.; Evain, E. J. *Tetrahedron* **1990**, *46*, 5055–5064.
(43) Jeyaraj, D. A.; Kapoor, K. K.; Yadav, V. K.; Gauniyal, H. M.; Parvez, M. *J. Org. Chem.* **1998**, *63*, 287–294.
(44) *Jaguar*, v.7.5;Schrödinger, LLC: New York, 2008.

**iqn**, which was found to be more stable than the coupled product $\mathbf{6^{Sc}}$-$\mathbf{py^{Ph}}$-**iqn** by 1.0 kcal/mol, in agreement with the experimental results. In order to evaluate the operating pathway, the corresponding transition structures and intermediates involved in each process were sought out.

The first pathway involved the migration of the proton to the amide nitrogen atom. On the basis of Mulliken charge comparison (−0.65 for N2, −0.94, and −0.96 for $N^{fc}$) and given its proximity to C2, this nitrogen atom could be basic enough to participate in or mediate the H transfer. However, this process involves an activation barrier $\Delta G^{\ddagger}$ of 60.0 kcal/mol, leading to an intermediate, $\mathbf{I_N}^{6-7}$, at 27.9 kcal/mol on the potential free energy surface (PES) relative to $\mathbf{6^{Sc}}$-$\mathbf{py^{Ph}}$-**iqn**. The transfer of the proton from N2 to C4 involves an even more improbable transition structure, which was estimated to be ca. 52 kcal/mol higher in energy than the intermediate $\mathbf{I_N}^{6-7}$. In addition, a pathway involving the ferrocene diamide ligand was explored. We found that this process also involves proton transfer via $\mathbf{I_N}^{6-7}$, as a consequence of the steric hindrance caused by the *tert*-butyldimethylsilyl groups, which prevents the biheterocyclic ligand from rotating and approaching the amidic N (or Sc) facially. On the basis of the high energies found for the two transition states, these mechanistic proposals were considered unrealistic.

Next, a metal-mediated isomerization was considered, in which $\beta$-hydride elimination to scandium occurs. A stationary point for the structure $\mathbf{I_H}^{6-7}$ was found at 24.7 kcal/mol on the PES. However, the ligand appears to be distorted (see the Supporting Information for details), and the hydride lies away from the source heterocycle. If such an intermediate were part of the isomerization, it is likely that reinsertion would occur into other aromatic groups, which was not observed experimentally. In addition, a direct transfer of H from C2 to Sc was not found computationally. All attempts to locate such a transition structure led to the intermediate $\mathbf{I_N}^{6-7}$ via the same 60.0 kcal/mol free energy activation barrier. Thus, it was concluded that the pathway is inoperative.

Finally, a direct pathway was considered. The proposed avenue involves a transition structure in which the heterocycle adopts a boat-like conformation. Such a conformation facilitates the direct proton transfer, leading to a free activation energy of $\Delta G^{\ddagger} = 29.9$ kcal/mol in benzene as a solvent. *Thus, it was concluded that the operating pathway is a direct transfer from C2 to C4* and that the driving force for the isomerization reactions of $\mathbf{6^{M}}$-$\mathbf{py^{Ph}}$-**iqn** to $\mathbf{7^{M}}$-$\mathbf{py^{Ph}}$-**iqn** is the increased stability (−1.0 kcal/mol for scandium) of the products $\mathbf{7^{M}}$-$\mathbf{py^{Ph}}$-**iqn**. It is also proposed that the small difference in stability between $\mathbf{6^{M}}$-$\mathbf{py^{Ph}}$-**iqn** and $\mathbf{7^{M}}$-$\mathbf{py^{Ph}}$-**iqn** explains why some reactions could not be driven to completion. To support this hypothesis, the gas-phase electronic energy differences between $\mathbf{6^{M}}$-$\mathbf{py^{Ph}}$-**iqn** and $\mathbf{7^{M}}$-$\mathbf{py^{Ph}}$-**iqn** were calculated from full geometry optimizations (using ADF2008.01), which led to −1.2 kcal/mol for Sc, −1.5 kcal/mol for Y, and −1.7 kcal/mol for Lu. By contrast, the compound $\mathbf{7^{Sc}}$-**qn-iqn** is more stable by 8.5 kcal/mol than $\mathbf{6^{Sc}}$-**qn-iqn**, reflected by the full conversion of $\mathbf{6^{Sc}}$-**qn-iqn** to $\mathbf{7^{Sc}}$-**qn-iqn**.

The same DFT methodology (B3LYP/LACV3P++**(2f)//B3LYP/LACVP**) was applied to the study of the ring-opening reaction of 1-methylimidazole described in Scheme 1 (Figure 3). Two pathways were investigated: one involving two and the other involving three 1-methylimidazole ligands. These pathways were based on the experimental observation that the reaction involving a total of 3 equiv of 1-methylimidazole is faster (5 h) than the one involving only 2 equiv (the reaction was 95% complete in 7 days). Starting from the compound $\mathbf{2^{Sc}}$-**imidazole**, the B3LYP[45−49] method of DFT predicts that the binding of a third equivalent of 1-methylimidazole is favored by 0.8 kcal/mol. The coupling of the 1-methylimidazolyl and of one of the coordinated 1-methylimidazole ligands to give $\mathbf{3^{Sc}}$ (21.6 kcal/mol) or $\mathbf{3^{Sc}}$-**imidazole** (4.8 kcal/mol) proceeds via transition structures at 32.9 and 21.1 kcal/mol, respectively.

In order to establish the pathway involving ring-opening to form the product $\mathbf{4^{Sc}}$, a relaxed coordinate scan was carried out starting from it ($\mathbf{4^{Sc}}$). In addition to the ring-opening step, the scan revealed that the dearomatized 1-methylimidazole fragment has to undergo a rotation to allow coordination of the nitrogen bearing the methyl group. Two cases were investigated:

(1) A rotation along the carbon−carbon bond between the coupled rings of $\mathbf{3^{Sc}}$-**imidazole** via a transition state at 33.6 kcal/mol allows the coordination of the nitrogen bearing the methyl group to form the intermediate $\mathbf{I_{Sc}}^{3-4}$-**imidazole** at 22.5 kcal/mol. The ring-opening process then occurs via a transition structure at 40.3 kcal/mol that rearranges to the product $\mathbf{4^{Sc}}$-**imidazole** (−2.3 kcal/mol).

(2) A similar rotation takes place for $\mathbf{3^{Sc}}$ via a transition state at 37.0 kcal/mol to allow the formation of the intermediate $\mathbf{I_{Sc}}^{3-4}$ at 27.4 kcal/mol. The ring-opening process then occurs via a transition structure at 40.3 kcal/mol that rearranges to the product $\mathbf{4^{Sc}}$ (−11.2 kcal/mol).

The results described above support the experimental observation that the reaction involving a total of 3 equiv of 1-methylimidazole is faster than the one involving only 2 equiv. The calculations led to the complex $\mathbf{2^{Sc}}$-**imidazole** as the resting state, as observed experimentally. All transition states and intermediates for the pathway involving 2 equiv of 1-methylimidazole are at least 5 kcal/mol higher in energy than those corresponding to the pathway involving 3 equiv, explaining the slower reaction rate observed when only 2 equiv of 1-methylimidazole was used. The final product, $\mathbf{4^{Sc}}$, forms after the ring-opened intermediate $\mathbf{4^{Sc}}$-**imidazole** loses a 1-methylimidazole ligand (a process favored by 8.9 kcal/mol).

Because the ring-opening of pyridine derivatives is relevant to HDN processes, the difference between the actual ring-opening of 1-methylimidazole and a hypothesized one for pyridine substrates was investigated computationally. The ring-opening of pyridine was proposed to start from the model complex $\mathbf{6^{Sc}}$-**py-py** (Figure 4), which represents the product of coupling between two pyridine rings. Two pathways were explored: (1) a rotation along C1−C2 and a disconnection at the newly formed C−C single bond which is directly analogous to the ring-opening of 1-methylimidazole (dashed lines in Figure 4), and (2) a breaking of the bond N2−C2 (Figure 1) between the amide nitrogen and the saturated carbon (solid lines in Figure 4).

The first pathway involves an activation barrier of 28.4 kcal/mol and leads to the intermediate $\mathbf{I_{Sc}}^{6-8}$ (24.0 kcal/mol).

(45) Becke, A. D. *J. Chem. Phys.* **1993**, *98*, 5648–5652.
(46) Becke, A. D. *Phys. Rev. A* **1988**, *38*, 3098.
(47) Vosko, S. H.; Wilk, L.; Nusair, M. *Can. J. Phys.* **1980**, *58*, 1200–1211.
(48) Lee, C.; Yang, W.; Parr, R. G. *Phys. Rev. B* **1988**, *37*, 785.
(49) Hertwig, R. H.; Koch, W. *Chem. Phys. Lett.* **1997**, *268*, 345–351.

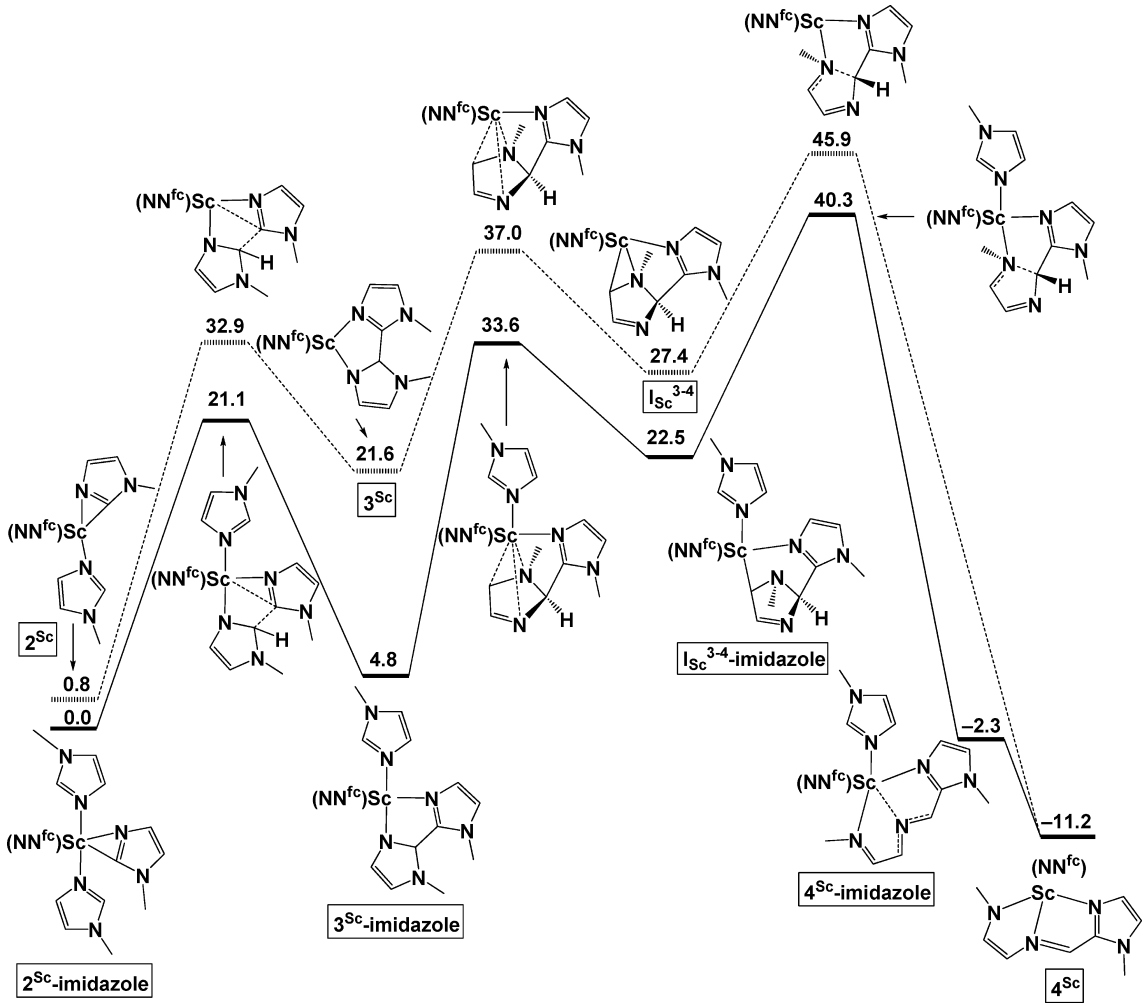


***Figure 3.*** Proposed mechanisms for the ring-opening of 1-methylimidazole by $\mathbf{1^{Sc}}$**-THF**; the dashed pathway involves only 2 equiv of 1-methylimidazole. Values are free energies ($\Delta G^{343K}$) (not drawn to scale) in kcal/mol and referenced to $\mathbf{2^{Sc}}$**-imidazole**.

Breaking the C−C single bond leads to the product $\mathbf{8^{Sc}}$ (24.7 kcal/mol) via a relative activation barrier of 38.1 kcal/mol. Such a high activation barrier makes it unlikely that this mechanism would take place as proposed. Alternatively, the second pathway, with the elongation of the N2−C2 bond, leads to the product $\mathbf{9^{Sc}}$ (22.3 kcal/mol) via an activation barrier of only 27.8 kcal/mol. The accessibility of the transition state for this pathway suggests that there may be reaction conditions that would lead to this process, provided that the ring-opened product can be stabilized versus the starting material.

## Conclusions

The reactions of two types of aromatic N-heterocycles (pyridines and imidazoles) with group III alkyl complexes were investigated experimentally and computationally. The two substrates form analogous biheterocyclic structures after the initial C−H activation event. However, in the case of 1-methylimidazole, the biheterocyclic compound could not be isolated and led to an imidazole ring-opened product. In the case of pyridines, a biheterocyclic product could be isolated and, by contrast, transformed into an isomer with extended conjugation of double bonds. The mechanism for the isomerization reaction was investigated both experimentally and computationally: experimentally, it was shown that the reaction proceeds intramolecularly, while DFT calculations established that the most likely pathway for the isomerization is a direct proton transfer between two carbons of the dearomatized pyridine ring. Given the importance of C−N bond cleavage in aromatic N-heterocycles, the ring-opening of 1-methylimidazole was also investigated computationally to establish similarities and differences with the reaction of pyridine substrates. It was concluded that the stability of the products is the most important factor in determining the different outcomes. DFT calculations carried out on mechanisms analogous to that for the ring-opening of 1-methylimidazole suggest that a pathway leading to the ring-opening of pyridines is energetically accessible, and, thus, experimental conditions may be found for the ring-opening of pyridines.

## Experimental Section

All experiments were performed under a dry nitrogen atmosphere using standard Schlenk techniques or an MBraun inert-gas glovebox. Solvents were purified using a two-column solid-state purification system by the method of Grubbs[50] and transferred to the glovebox without exposure to air. NMR solvents were obtained from Cambridge Isotope Laboratories,

(50) Pangborn, A. B.; Giardello, M. A.; Grubbs, R. H.; Rosen, R. K.; Timmers, F. J. *Organometallics* **1996**, *15*, 1518–1520.

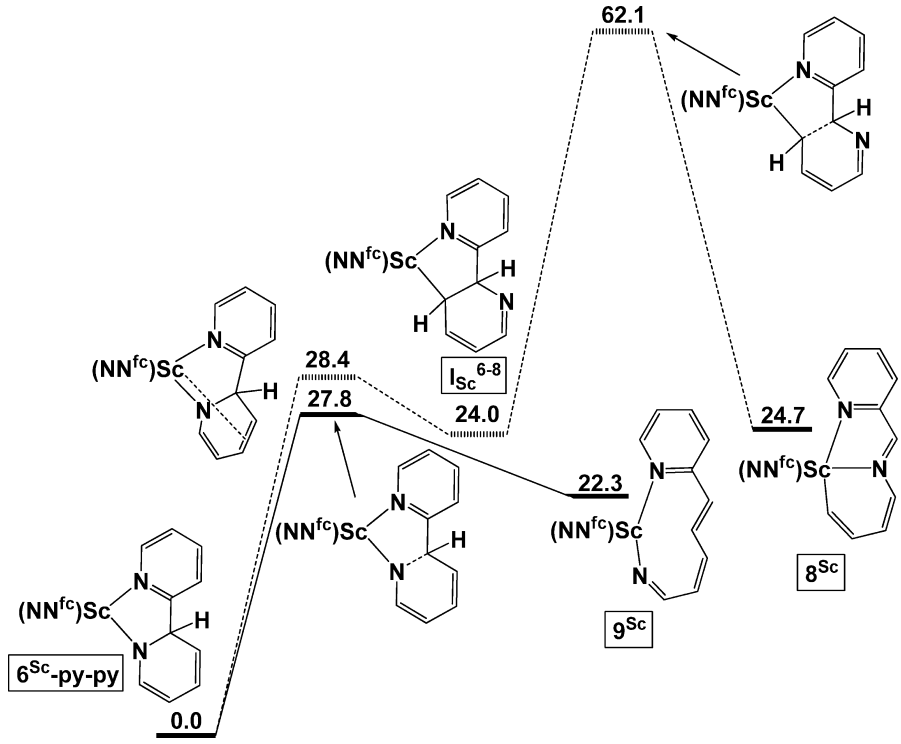


***Figure 4.*** Proposed mechanisms for the ring-opening of pyridine by **1$^{Sc}$-THF**. All energies (not drawn to scale) are given in kcal/mol and referenced to **6$^{Sc}$-py-py**.

degassed, and stored over activated molecular sieves prior to use. Scandium, yttrium, and lutetium oxides were purchased from Stanford Materials Corp. (Aliso Viejo, CA) and used as received. K(CH$_2$Xy-3,5), KCH$_2$Ph, **1$^{Sc}$-THF**, **1$^{Y}$-THF**, and **5$^{Sc}$-py$^{Ph}$** were prepared following published procedures.[27] The aromatic heterocycles were distilled or recrystallized before use; all other materials were used as received. $^1$H NMR spectra were recorded on Bruker300, Bruker500, or Bruker600 spectrometers (work supported by the NSF grant CHE-9974928) at room temperature in $C_6D_6$ unless otherwise specified. Chemical shifts are reported with respect to internal solvent, 7.16 ppm ($C_6D_6$). CHN analyses were performed at the UC Berkeley Micro-Mass Facility (College of Chemistry, University of California, Berkeley).

**Synthesis of 5$^{Sc}$-qn.** The compound **1$^{Sc}$-THF** (300 mg, 0.442 mmol) was combined with 1.05 equiv of 8-methylquinoline (66.4 mg, 0.464 mmol) in toluene (8 mL) and stirred for 4 h at room temperature. The solvent was removed, the resulting red-orange solid extracted in hexanes, the solution filtered through Celite, and the filtrate concentrated and placed in a −35 °C freezer. Yield: 253.2 mg, 81.5% as two crops of crystals from hexanes.

$^1$H NMR (500 MHz, $C_6D_6$), $\delta$ (ppm): 7.97 (d, 1H, quinoline), 7.72 (d, 1H, quinoline), 7.42 (t, 1H, quinoline), 7.33 (t, 1H, quinoline), 7.18 (t, 1H, quinoline), 4.25 (s, 2H, fc-C*H*), 4.21 (s, 4H, OC*H*$_2$CH$_2$), 4.11 (s, 2H, fc-C*H*), 3.73 (s, 2H, fc-C*H*), 4.11 (s, 2H, fc-C*H*), 3.28 (s, 2H, fc-C*H*), 3.00 (s, 3H, quinoline-C*H*$_3$), 1.52 (s, 4H, OCH$_2$C*H*$_2$), 0.82 (s, 18H, SiC(C*H*$_3$)$_3$), −0.14 and −0.42 (s, 6H, SiC*H*$_3$). $^{13}$C NMR (126 MHz, $C_6D_6$), $\delta$ (ppm): 144.2, 133.6, 133.4, 130.0, 129.0, 127.0, 126.6, 125.9, 101.4, 72.8, 68.2, 68.1, 67.5, 66.3, 27.7, 25.4, 20.2, 19.1, −2.3, −3.1. Anal. Calcd for $C_{36}H_{55}FeN_3OScSi_2$: C, 61.52; H, 7.89; N, 5.98. Found: C, 61.72; H, 7.68; N, 5.63.

**Synthesis of 5$^{Y}$-py$^{Ph}$.** The compound **1$^{Y}$-THF** (0.2204 g, 0.323 mmol) was combined with 0.95 equiv of 2-phenylpyridine (0.0475 g, 0.306 mmol) in toluene (10 mL) and stirred for 1 h at 50 °C. The solvent was removed under reduced pressure, and the resulting dark green solid was dissolved in minimal pentane (ca. 2 mL) and left overnight to precipitate a dark yellow-green solid. Yield: 0.1394 mg, 60.1%.

$^1$H NMR (500 MHz, $C_6D_6$), $\delta$ (ppm): 8.02−7.97 (m, 3H, NC$_5$*H*$_3$), 7.36−7.26 (m, 5H, py-C$_6$*H*$_5$), 4.14 (s, 2H, fc-C*H*), 4.06 (s, 4H, OC*H*$_2$CH$_2$), 3.50 (s, 2H, fc-C*H*), 3.43 (s, 2H, fc-C*H*), 1.41 (t, 4H, OCH$_2$C*H*$_2$), 0.86 (s, 18H SiC(C*H*$_3$)$_3$), −0.07 (s, 12H, Si(C*H*$_3$)$_2$). $^{13}$C NMR (126 MHz, $C_6D_6$), $\delta$ (ppm): 220.4, 153.4, 139.3, 134.2, 129.8, 128.7, 128.3, 126.9, 118.7, 104.8, 71.5, 66.2, 34.1, 32.1, 27.1, 25.0, 22.4, 19.8, 13.9, −3.2. Anal. Calcd for $C_{37}H_{54}FeN_3OYSi_2$: C, 58.65; H, 7.18; N, 5.54. Found: C, 59.04; H, 7.48; N, 5.21.

**Synthesis of 5$^{Lu}$-py$^{Ph}$.** The compounds **1$^{Lu}$-THF** (0.1663 g, 0.206 mmol) and 2-phenylpyridine (0.0317 g, 0.204 mmol) were combined in a Schlenk tube with 5 mL of uene. The resultant bright orange solution was heated at 70 °C for ∼2 h until the solution had a dark brown color. The solution was then dried under vacuum,and the resultant solid was taken up in *n*-pentane and filtered through Celite. The filtrate was concentrated under vacuum and stored at −35 °C overnight, giving brown-orange crystals. Yield: 0.1193 g, 62.9%.

$^1$H NMR (500 MHz, $C_6D_6$), $\delta$ (ppm): 8.10 and 8.09 (d, 2H, pyridyl), 7.98 and 7.96 (d, 1H, pyridyl), 7.38−7.18 (m, 5H, py-C$_6$*H*$_5$), 4.13 (br, 8H, both OC*H*$_2$CH$_2$ and fc-C*H*), 3.68 and 3.35 (br, 4H, fc-C*H*), 1.43 (br, 4H, OCH$_2$C*H*$_2$), 0.85 (s, 18H, SiC(C*H*$_3$)$_3$), −0.10 (s, 12H, (Si(C*H*$_3$)$_2$)$_2$. $^{13}$C NMR (126 MHz, $C_6D_6$), $\delta$ (ppm): 229.5, 154.1, 139.3, 135.2, 130.7, 129.3, 128.8, 128.6, 127.4, 119.2, 104.1, 72.4, 66.5, 27.5, 25.4, 20.3, 14.4, −2.8. Anal. Calcd for $C_{37}H_{54}N_3OSi_2FeLu$: C, 52.66; H, 6.45; N, 4.98. Found: C, 52.11; H, 6.67; N, 4.80.

**Synthesis of 6$^{Sc}$-py$^{Ph}$-iqn.** The compound **5$^{Sc}$-py$^{Ph}$** (0.3000 g, 0.420 mmol) was combined with 1.1 equiv of 3-methylisoquinoline (0.0662 g, 0.4263 mmol) in toluene (10 mL). The reaction mixture was stirred for 3 h at room temperature. The solvent was removed, and the resulting blood red solid was washed with hexanes and extracted in toluene. Yield: 0.2633 g, 79.8% as crystals from toluene:pentane at −35 °C.

$^1$H NMR (500 MHz, $C_6D_6$), $\delta$ (ppm): 7.66 (d, 2H, aryl), 7.30−7.19 (m, 4H, aryl), 7.16−7.05 (m, 4H, aryl), 6.94 (d, 1H, aryl), 6.78 (d, 1H, aryl), 5.80 (s, 1H, isoquinoline-N-C*H*), 5.75 (s, 1H, olefinic), 4.23 (s, 1H, fc-C*H*), 4.06 (s, 1H, fc-C*H*), 3.92

(s, 1H, fc-C*H*), 3.89 (s, 1H, fc-C*H*), 3.36 and 3.36 (s, 1H, fc-C*H*), 3.28 (s, 1H, fc-C*H*), 3.27 (s, 1H, fc-C*H*), 2.18 (s, 1H, fc-C*H*), 2.18 (s, 3H, isoquin-C$H_3$), 0.83 and 0.77 (s, 9H, SiC(C$H_3$)$_3$), 0.00 (s, 6H, SiC$H_3$), −0.12 and −0.36 (s, 3H, SiC$H_3$). $^{13}$C NMR (126 MHz, $C_6D_6$), $\delta$ (ppm): 164.6, 158.3, 152.5, 139.5, 139.1, 138.2, 130.6, 130.1, 127.6, 127.2, 126.1, 125.5, 122.8, 122.5, 122.4, 121.4 99.7, 99.3, 97.2, 69.7, 68.9, 68.4, 68.0, 67.5, 68.0, 67.4, 67.1, 66.8, 27.7, 27.5, 22.7, 20.0, 19.9, −2.6, −2.8, −4.3. $\lambda_{max}$/nm ($\varepsilon$/M$^{-1}$ cm$^{-1}$) = 286 (15 800), 332 (11 700). Anal. Calcd for $C_{43}H_{55}FeN_4ScSi_2$·toluene: C, 68.47; H, 7.23; N, 6.38. Found: C, 68.16; H, 7.41; N, 6.70.

**Synthesis of 6$^{Sc}$-qn-iqn.** The compound **5$^{Sc}$-qn** (0.2000 g, 0.285 mmol) was combined with 1.1 equiv of 3-methylisoquinoline (0.0448 g, 0.313 mmol) in toluene (10 mL) and stirred for 2 h at room temperature. The solvent was removed, and the blood red solid was washed with hexanes and extracted in toluene. Yield: 0.1476 g, 67.12% as the first crop of crystals from toluene: pentane. Crystals suitable for X-ray diffraction were obtained from toluene:pentane at −35 °C; however, upon cooling to 110 K the crystals shattered, preventing full crystallographic analysis.

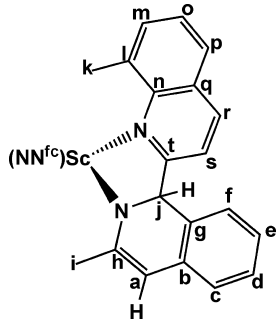


$^1$H NMR (500 MHz, $C_6D_6$), $\delta$ (ppm): 7.46 (d, 1H, s), 7.26 (tr, 1H, e), 7.25 (tr, 1H, d), 7.21 (d, 1H, r), 7.13 (d, 1H, c), 7.11 (d, 1H, m), 7.06 (tr, 1H, o), 6.85 (d, 1H, f), 5.86 (s, 1H, j), 5.84 (s, 1H, a), 4.22 (s, 1H, fc-C*H*), 4.18 (s, 1H, fc-C*H*), 4.06 (s, 1H, fc-C*H*), 4.05 (s, 1H, fc-C*H*), 3.41 (s, 1H, fc-C*H*), 3.37 (s, 1H, fc-C*H*), 3.27 (s, 1H, fc-C*H*), 3.21 (s, 1H, fc-C*H*), 3.01 (s, 3H, quin-C$H_3$), 2.26 (s, 3H, isoquin-C$H_3$), 0.76 and 0.62 (s, 9H, SiC(C$H_3$)$_3$), −0.14, −0.15, −0.21, and −0.43 (s, 3H, SiC$H_3$). $^{13}$C NMR (126 MHz, $C_6D_6$), $\delta$ (ppm): 167.4 (t), 152.8 (h), 145.8 (l), 139.7 (b or g), 139.3 (s), 132.0 (q or n), 127.4 (r), 127.1 (e), 127.0, 126.4 (b or g), 124.3 (c), 123.1 (f), 122.5 (o), 121.6 (d), 99.0 and 98.5 (fc-*C*-N), 97.4 (a), 69.3, 69.0, 68.8, 68.5, 68.2, 68.0, 67.9, and 67.7 (fc-*C*H), 27.5 and 27.3 ([SiC(*C*H$_3$)$_3$]$_2$), 22.8 (i), 19.9 and 19.8 ([Si*C*(CH$_3$)$_3$]$_2$), 18.5 (k), −2.7, −3.0, −3.8, and −4.0 ([Si(*C*H$_3$)$_2$]$_2$). $\lambda_{max}$/nm ($\varepsilon$/M$^{-1}$ cm$^{-1}$) = 236 (81 400), 320 (34 900), 362 (22 300), 526 (1810). Anal. Calcd for [$C_{42}H_{55}FeN_4ScSi_2$]$_2$·toluene: C, 66.73; H, 7.26; N, 6.84. Found: C, 66.90; H, 7.30; N, 6.53.

**Synthesis of 6$^{Y}$-py$^{Ph}$-iqn.** The compound **5$^{Y}$-py$^{Ph}$** (0.0873 g, 0.115 mmol) was combined with 3 equiv of 3-methylisoquinoline (0.0545 g, 0.381 mmol) in $C_6D_6$ (4 mL) and stirred for 2 h at room temperature. The solvent was removed by vacuum, and the resulting dark red oil was dissolved in minimal hexanes (ca. 3 mL) and left overnight at −35 °C to precipitate dark red crystals. Yield: 0.0693 g, 72.7%.

$^1$H NMR (300 MHz, $C_6D_6$), $\delta$ (ppm): 7.53 (m, 2H, q and u), 7.28 (m, 4H, m,r,s,t), 7.08 (m, 2H, f,g), 6.99 (m, 2H, e,h), 6.83 (d, 1H, n), 6.78 (d, 1H, l), 5.88 (s, 1H, j), 5.65 (s, 1H, c), 4.16 (s, 1H, fc-C*H*), 4.10 (s, 1H, fc-C*H*), 3.91 (s, 1H, fc-C*H*), 3.81 (s, 1H, fc-C*H*), 3.30 (s, 1H, fc-C*H*), 3.27 (s,1H, fc-C*H*), 3.22 (s, 1H, fc-C*H*), 1.97 (s, 1H, fc-C*H*), 2.19 (s, 3H, a), 0.89 (s, 9H, SiC(C$H_3$)$_3$), 0.75 (s, 9H, SiC(C$H_3$)$_3$), 0.01 (s, 3H, Si(C$H_3$)$_2$), −0.02 (s, 3H, Si(C$H_3$)$_2$), −0.06 (s, 3H, Si(C$H_3$)$_2$), −0.39 (s, 3H, Si(C$H_3$)$_2$). $^{13}$C NMR (126 MHz, $C_6D_6$), $\delta$ (ppm): 165.9, 165.9, 156.9, 152.9, 139.5, 139.3, 138.2, 132.4, 130.3, 128.2, 126.9,

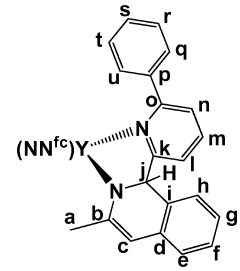


126.0, 125.7, 125.3, 122.2, 122.0, 121.0, 120.7, 103.1, 103.0, 96.7, 68.6, 68.3, 68.2, 67.9, 67.7, 66.9, 66.8, 66.5, 65.2, 31.8, 27.4, 27.3, 26.5, 22.9, 22.2, 19.85, 19.82, 14.2, −2.9, −3.0, −3.1, −4.5. Anal. Calcd for $C_{42}H_{55}FeN_4YSi_2$: C, 62.31; H, 6.69; N, 6.76. Found: C, 62.15; H, 6.79; N, 6.38.

**Synthesis of 6$^{Lu}$-py$^{Ph}$-iqn.** The compound **5$^{Lu}$-py$^{Ph}$** (0.1193 g, 0.128 mmol) was combined with 3-methylisoquinoline (0.0546 g, 0.381 mmol) in ∼3 mL of toluene. The solution was stirred at room temperature for 2 h. The red solution was then dried under vacuum, leaving a red powder. The solid was taken up in hexanes and filtered through Celite. The filtrate was concentrated under vacuum and cooled to −35 °C to afford red crystals of **6$^{Lu}$-py$^{Ph}$-iqn**. Yield: 0.0720 g, 62.0%. Average yield for this reaction: 70%. *Note*: The percent yield was larger when the reaction was done on a smaller scale.

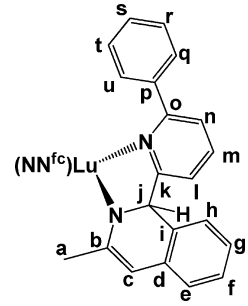


$^1$H NMR (500 MHz, $C_6D_6$), $\delta$ (ppm): 7.67 and 7.65 (d, 2H, r and t), 7.31 (t, 2H, q and u), 7.27, 7.26 (d, 1H, l), 7.24 (t, 1H, m), 7.08 (s, 1H, n), 7.07 (s, 1H, h), 7.04 (d, 1H, s), 7.03 (d, 1H, e), 6.83, 6.81, 6.78, 6.77 (d of d, 2H, f and g), 5.88 (s, 1H, j), 5.63 (s, 1H, c), 4.14, 4.06, 3.89, 3.80, 3.39, 3.36, 3.32, 2.07 (s, 1H each, fc-*H*), 2.26 (s, 3H, a), 0.87 (s, 9H, SiC(C$H_3$)$_3$), 0.75 (s, 9H, SiC(C$H_3$)$_3$), −0.00 (s, 3H, Si(C$H_3$)), −0.01 (s, 3H, Si(C$H_3$)), −0.11 (s, 3H, Si(C$H_3$)), −0.43 (s, 3H, Si(C$H_3$)). $^{13}$C NMR (126 MHz, $C_6D_6$), $\delta$ (ppm): 165.5 (d,i), 157.3 (o), 153.0. (b), 139.6 (h), 138.2 (p), 132.5 (q,u), 130.5 (s), 127.1 (l) 126.02 (k), 125.97 (r and t), 125.7 (e), 122.42 (n), 122.38, 121.5 (f and g), 121.3 (m), 102.3 (fc-*C*), 97.9 (j), 68.41, 68.26, 68.00, 67.41, 67.33, 66.36, 65.82, 65.37 (fc-*C*H), 67.5 (c), 36.3 and 34.8 (*t*Bu-*C*(CH$_3$)$_3$), 27.6 and 27.3 (*t*Bu-C(*C*H$_3$)$_3$), 22.6 (a), −2.80, −2.89, −2.97, −4.50 ([Si(*C*H$_3$)$_2$]$_2$). Anal. Calcd for $C_{43}H_{55}N_4Si_2FeLu$: C, 56.45; H, 6.06; N, 6.12. Found: C, 56.33; H, 6.29; N, 5.78.

**Synthesis of 7$^{Sc}$-qn-iqn.** The compound **6$^{Sc}$-qn-iqn** (0.2600 g, 0.336 mmol) was dissolved in toluene (10 mL) and stirred at 70 °C for 96 h. After 12 h the solution turned dark purple. The solvent was removed, and the resulting purple solid was filtered in hexanes. Yield: 0.1953 g, 75.12%. Crystals suitable for X-ray diffraction were grown from a solution of $Et_2O$:pentane at −35 °C.

$^1$H NMR (500 MHz, $C_6D_6$), $\delta$ (ppm): 7.94 (d, 1H, c), 7.48 (d, 1H, r), 7.17 (tr, 1H, e), 7.07 (tr, 1H, d), 6.92 (d, 2H, m,p), 6.89 (d, 1H, f), 6.76 (d, 1H, s), 6.73 (tr, 1H, o), 4.17 (s, 2H, fc-C*H*), 4.08 (s, 2H, fc-C*H*), 3.24 (s, 2H, fc-C*H*), 3.19 (s, 2H, fc-C*H*), 3.14 (s, 2H, a), 2.71 (s, 3H, k), 1.96 (s, 3H, i), 0.81 (s, 18H, SiC(C$H_3$)$_3$), 0.09 and 0.06 (s, 6H, SiC$H_3$). $^{13}$C NMR (126 MHz, $C_6D_6$), $\delta$ (ppm): 150.7 (t), 149.6 (h), 148.8 (l), 133.8 (s), 132.3 (g), 130.7 (m), 127.2 (f), 127.0 (e), 126.8 (p), 125.7 (b), 124.9 (d), 123.6 (l), 123.3 (q), 122.7 (r), 120.8

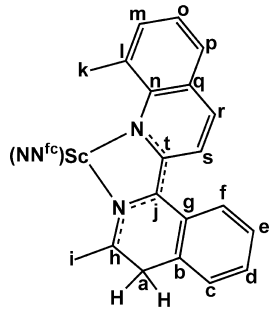


(c), 119.6 (o), 116.4 (j), 97.8 (fc-*C*-N), 69.3 (fc-*C*-H), 68.7 (fc-*C*-H), 68.3 (fc-*C*-H), 67.8 (fc-*C*-H), 38.5 (a), 27.4 (SiC(*C*H$_3$)$_3$), 25.4 (i), 19.9 (Si*C*(CH$_3$)$_3$), 19.2, (k), −3.4 (Si*C*H$_3$), −3.8 (Si*C*H$_3$). $\lambda_{max}$/nm ($\varepsilon$/M$^{-1}$ cm$^{-1}$) = 250 (37 200), 292 (28 500), 758 (790), 832 (1210), 938 (1190). Anal. Calcd for $C_{42}H_{55}FeN_4ScSi_2$: C, 65.26; H, 7.17; N, 7.24. Found: C, 64.97; H, 7.22; N, 7.17.

**Synthesis of 7$^{Sc}$-py$^{Ph}$-iqn.** The compound **5$^{Sc}$-py$^{Ph}$** (0.2000 g, 0.281 mmol) was combined with 1.1 equiv of 3-methylisoquinoline (0.0441 mg, 0.308 mmol) in toluene (10 mL) and stirred at 70 °C for 10 days. After 12 h the solution turned dark green. The solvent was removed, and the resulting green solid was extracted in hexanes. Monitoring the reaction in a J-Young tube by $^1$H NMR spectroscopy revealed that too much decomposition of **7$^{Sc}$-py$^{Ph}$-iqn** occurred by the time all of the **6$^{Sc}$-py$^{Ph}$-iqn** was converted. Therefore, the reaction was stopped when the ratio of **7$^{Sc}$-py$^{Ph}$-iqn**:**6$^{Sc}$-py$^{Ph}$-iqn** was ca. 5:1. Yield: 0.0959 g, 43.6% as crystals from hexanes.

$^1$H NMR (600 MHz, $C_6D_6$), $\delta$ (ppm): 8.06 (d, 1H, aryl), 7.71 (d, 2H, aryl), 7.40 (d, 1H, aryl), 7.25−7.16 (m, 2H, aryl), 7.10−6.92 (m, 4H, aryl), 6.65 (d, d 1H, aryl), 5.68 (d, 1H, aryl), 4.08 (s, 2H, fc-C*H*), 4.00 (s, 2H, fc-C*H*), 3.20 (s, 2H, C*H*$_2$), 3.13 (s, 2H, fc-C*H*), 2.81 (s, 2H, fc-C*H*), 1.88 (s, 3H, C−C*H*$_3$), 0.83 (s, 18H, SiC(C*H*$_3$)$_3$), 0.24 and 0.14 (s, 6H, SiC*H*$_3$). $^{13}$C NMR (151 mHz, $C_6D_6$), $\delta$ (ppm): 155.7, 153.8, 142.0, 135.9, 132.9, 131.4, 127.2, 127.3, 126.9,125.6, 123.9, 123.7, 118.5, 117.8, 112.4, 106.2, 98.8, 69.5, 68.8, 68.5, 67.6, 38.5, 27.6, 25.2, 20.1, −3.1, −3.9. $\lambda_{max}$/nm ($\varepsilon$/M$^{-1}$ cm$^{-1}$) = 280 (10 100), 342 (5060), 412 (9910), 458 (5960), 600 (3880). Anal. Calcd for $C_{43}H_{55}FeN_4ScSi_2$: C, 65.80; H, 7.06; N, 7.14. Found: C, 65.57; H, 7.28; N, 7.26.

**Synthesis of 7$^{Sc}$-qn-pic.** The compound **5$^{Sc}$-qn** (0.2000 g, 0.285 mmol) was combined with 1.1 equiv of 2-picoline (0.0292 mg, 0.313 mmol) in toluene (10 mL). The reaction was heated at 70 °C for 4 days. The solvent was removed, and the resulting brown solid was extracted in hexanes. Yield: 0.1523 g, 74.0%. Attempts to isolate the **6$^{Sc}$-qn-pic** product were unsuccessful because the coupling reaction is competitive with the isomerization one.

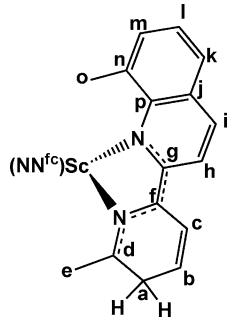


$^1$H NMR (500 MHz, $C_6D_6$), $\delta$ (ppm): 7.33 (d, 1H, h), 6.93 (m, 2H, two of i, k, l, or m), 6.91 (m, 1H, c), 6.81 (tr, 1H, i, k, l, or m), 6.33 (d, 1H, i, k, l, or m), 5.50 (tr, 1H, b), 4.23 (s, 2H, fc-C*H*), 4.05 (s, 4H, fc-C*H* and a), 3.30 (s, 4H, fc-C*H*), 2.75 (s, 3H, e), 2.36 (s, 3H, o), 0.83 (s, 18H, SiC(C*H*$_3$)$_3$), −0.02 and −0.11 (s, 6H, SiC*H*$_3$). $^{13}$C NMR (126 MHz, $C_6D_6$), $\delta$ (ppm): 159.4 (g), 154.4 (n), 148.6 (d), 144.0 (p or j), 138.5 (i, k, l, or m), 123.3 (p or j), 121.4 (i, k, l, or m), 119.9 (i, k, l, or m), 118.3 (f), 117.8 (h), 102.2 (b), 98.1 (fc-*C*-N), 69.2, 68.7, 68.4 and 66.9 (fc-*C*H), 30.0 (a), 27.5 (SiC(*C*H$_3$)$_3$), 23.2 (o), 21.1 (e), 19.9 (Si*C*(CH$_3$)$_3$), −3.6 and −3.8 (Si(*C*H$_3$)$_2$. $\lambda_{max}$/nm ($\varepsilon$/M$^{-1}$ cm$^{-1}$) = 250 (37 300), 294 (28 200), 390 (9740), 446 (8290), 740 (1410), 822 (1620), 926 (1420). Anal. Calcd for $C_{38}H_{53}FeN_4ScSi_2$: C, 63.14; H, 7.39; N, 7.75. Found: C, 63.80; H, 7.67; N, 7.76.

**DBU-Catalyzed Isomerization.** The compound **6$^{Sc}$-qn-iqn** (60 mg, 0.078 mmol) was combined with 1.3 equiv of DBU (15.4 mg, 0.100 mmol) in $C_6D_6$ (0.5 mL); 95% conversion to **7$^{Sc}$-qn-iqn** was observed within 20 min.

The compound **6$^{Sc}$-py$^{Ph}$-iqn** (30 mg, 0.039 mmol) was combined with DBU (1.2 mg, 0.0078 mmol, 20 mol %) in $C_6D_6$; 75% conversion to **7$^{Sc}$-py$^{Ph}$-iqn** was observed after 8 h. Addition of excess DBU did not change the final ratio of **6$^{Sc}$-py$^{Ph}$-iqn** to **7$^{Sc}$-py$^{Ph}$-iqn**.

**Deuterium Labeling Experiment.** The compound **5$^{Sc}$-qn** (0.1000 g, 0.1422 mmol) was combined with 1 equiv of deuterated 3-methylisoquinoline (0.0207 g, 0.1422 mmol) in $C_6D_6$ (1.5 mL) and allowed to stand overnight at room temperature. The next day, the $C_6D_6$ solution was divided into equal portions, the solvent was removed from one of them, and the obtained solid was dissolved in $C_6H_6$. The two reactions were heated simultaneously at 70 °C and monitored by $^1$H and $^2$H NMR spectroscopy, respectively. After 6 days, the solvents were switched, and the complementary NMR spectra were collected.

**Crossover Experiment.** A mixture of **6$^{Sc}$-py$^{Ph}$-iqn** (0.0250 g, 0.032 mmol) and **6$^{Sc}$-qn-iqn** -$d_4$ (0.0250 g, 0.032 mmol) was dissolved in $C_6D_6$ (1 mL); a second portion of the same mixture was dissolved in $C_6H_6$. These two samples were heated to 70 °C (eq 1) while monitoring by $^1$H and $^2$H NMR spectroscopy, respectively. No deuterium incorporation into **7$^{Sc}$-py$^{Ph}$-iqn** was observed over the course of the isomerization of **6$^{Sc}$-qn-iqn**-$d_4$ to **7$^{Sc}$-qn-iqn**-$d_4$.

**X-ray Crystal Structure of 6$^{Sc}$-py$^{Ph}$-iqn.** X-ray-quality crystals were obtained from a concentrated toluene:pentane solution placed in a −35 °C freezer in the glovebox. A total of 11 280 reflections ($-21 \le h \le 21$, $-13 \le k \le 13$, $-36 \le l \le 36$) were collected at $T$ = 100(2) K with $2\theta_{max}$ = 56.57°, of which 6454 were unique ($R_{int}$ = 0.1123). The residual peak and hole electron density were 0.44 and −0.43 e A$^{-3}$, respectively. The least-squares refinement converged normally with residuals of $R_1$ = 0.0544 and GOF = 0.992. One molecule of toluene solvent was found in the unit cell. Crystal and refinement data for **3$^{Sc}$-py$^{Ph}$-iqn**: formula $C_{50}H_{63}N_4Si_2FeSc$, space group $P2(1)/c$, $a$ = 16.1271(19), $b$ = 10.5039(13), and $c$ = 27.189(3) Å, $\beta$ = 95.680(1)°, $V$ = 4583.2(10) Å$^3$, $Z$ = 4, $\mu$ = 0.555 mm$^{-1}$, $F(000)$ = 1864, $R_1$ = 0.1187 and $wR_2$ = 0.1237 (based on all 11280 data, $I > 2\sigma(I)$).

**X-ray Crystal Structure of 7$^{Sc}$-py$^{Ph}$-iqn.** X-ray-quality crystals were obtained from a concentrated $Et_2O$:pentane solution placed in a −35 °C freezer in the glovebox. A total of 9528 reflections ($-22 \le h \le 22$, $-18 \le k \le 18$, $-24 \le l \le 24$) were collected at $T$ = 100(2) K with $2\theta_{max}$ = 56.07°, of which 6056 were unique ($R_{int}$ = 0.0828). The residual peak and hole electron density were 0.42 and −0.45 e A$^{-3}$. The least-squares refinement converged normally with residuals of $R_1$ = 0.0447 and GOF = 1.012. Crystal and refinement data for **7$^{Sc}$-py$^{Ph}$-iqn**: formula $C_{43}H_{55}N_4Si_2FeSc$, space group $P2(1)/c$, $a$ = 16.782(3), $b$ = 13.647(2), and $c$ = 18.368(3) Å, $\beta$ = 109.108(2)°, $V$ = 3975.0(11) Å$^3$, $Z$ = 4, $\mu$ = 0.632 mm$^{-1}$, $F(000)$ = 1664, $R_1$ = 0.0902 and $wR_2$ = 0.1197 (based on all 9528 data, $I > 2\sigma(I)$).

**Computational Details.** Calculations were performed using density functional theory (DFT). For the mechanistic investigations, the B3LYP functional (as implemented in Jaguar 7.5, release 207) with the 6-311++G** basis set[51] for the main group atoms was employed. Small core effective potentials (angular momentum

(51) Krishnan, R.; Binkley, J. S.; Seeger, R.; Pople, J. A. *J. Chem. Phys.* **1980**, *72*, 650–654.

projected pseudopotentials) were used for Fe and Sc.[52−54] The basis set for Fe and Sc was LACV3P++**(2f), which includes a double-ζ f-shell into the LACV3P++** basis set.[55]

All structures were optimized in the gas phase (starting with geometries obtained from the X-ray crystal structures) using the LACVP** and 6-31G** basis sets.[52,56] For stationary points and transition structures, the analytic Hessian was calculated to obtain vibrational frequencies, which in turn were used to obtain zero-point and vibrational thermodynamic corrections (ZPE, $H(T)$, and $S$) to 343 K.

Solvent corrections were based on single-point self-consistent Poisson−Boltzmann continuum solvation calculations for benzene ($\varepsilon = 2.284$ and $R_0 = 2.60$ Å) using the PBF module in Jaguar.[57,58]

The calculations using the Amsterdam Density Functional (ADF) package (version ADF2008.01)[59−61] used the BLYP functional for full geometry optimizations and the B3LYP functional for single-point calculations on the geometries calculated with the BLYP functional. For all atoms, standard triple-ζ STA basis sets from the ADF database ZORA/TZP were employed.

**Acknowledgment.** P.L.D. thanks Prof. Jennifer A. Love, University of British Columbia, for a useful suggestion, Dr. Saeed Khan, UCLA, for help with some crystallography details, and Dr. Robert Taylor for help with NMR experiments. D.B. and E.T. thank Dr. Robert J. Nielsen for helpful suggestions. The experimental work was supported by UCLA. The MSC computational facilities were funded by grants from ARO-DURIP and ONR-DURIP.

**Supporting Information Available:** Experimental details for compound characterizations, DFT calculation details, and full crystallographic descriptions (CIF). This material is available free of charge via the Internet at http://pubs.acs.org.

JA902794W

(52) Hay, P. J.; Wadt, W. R. *J. Chem. Phys.* **1985**, *82*, 299–310.
(53) Melius, C. F.; Goddard, W. A. *Phys. Rev. A* **1974**, *10*, 1541.
(54) Melius, C. F.; Olafson, B. D.; Goddard, W. A. *Chem. Phys. Lett.* **1974**, *28*, 457–462.
(55) Martin, J. M. L.; Sundermann, A. *J. Chem. Phys.* **2001**, *114*, 3408–3420.
(56) Ditchfield, R.; Hehre, W. J.; Pople, J. A. *J. Chem. Phys.* **1971**, *54*, 724–728.
(57) Tannor, D. J.; Marten, B.; Murphy, R.; Friesner, R. A.; Sitkoff, D.; Nicholls, A.; Honig, B.; Ringnalda, M.; Goddard, W. A. *J. Am. Chem. Soc.* **1994**, *116*, 11875–11882.
(58) Marten, B.; Kim, K.; Cortis, C.; Friesner, R. A.; Murphy, R. B.; Ringnalda, M. N.; Sitkoff, D.; Honig, B. *J. Phys. Chem.* **1996**, *100*, 11775–11788.
(59) *ADF2008.01*, SCM; Theoretical Chemistry, Vrije Universiteit: Amsterdam, The Netherlands; 2008; http://www.scm.com.
(60) te Velde, G.; Bickelhaupt, F. M.; Baerends, E. J.; Fonseca Guerra, C.; van Gisbergen, S. J. A.; Snijders, J. G.; Ziegler, T. *J. Comput. Chem.* **2001**, *22*, 931–967.
(61) Fonseca Guerra, C.; Snijders, J. G.; te Velde, G.; Baerends, E. J. *Theor. Chem. Acc.* **1998**, *99*, 391–403.